CL2

X-RAY DIFFRACTION SYSTEMS – TECHNICAL ADVANTAGES AND APPLICATION RELATED BENEFITS

Lukasz Sadowski

STOE & Cie GmbH, info@stoe.com

Experimental factors such as crystal characteristics, available experiment time and the properties of the X-ray sources and detectors have a strong impact on data quality and can make the difference between success and failure in phasing attempts or result in a more or less accurate atomic model. The talk focuses on the XRD equipment and is intended as an overview on recent developments of X-ray diffraction systems and the fields where STOE XRD instruments are most beneficial.

A variety of measurement setups with respect to goniometers, diffraction geometries, detectors, X-ray sources and sample environments will be presented, and both Powder XRD and Single Crystal XRD applications will be exemplified. Additionally, recent advances in detector technology, novel in situ camera and implementation of MetalJet X-ray source will be highlighted and the tangible benefits for the scientists will be made transparent, e.g. gaining measurement speed, improving data quality and acceptance of samples with complex crystallinity.

Session V, Tuesday, June 19

L14

STRUCTURAL DESCRIPTION AND PROPERTIES OF Mg_2Al-LAYERED DOUBLE HYDROXIDES INTERCALATED WITH THE FLUVASTATIN ANIONS SOLVED BY MOLECULAR SIMULATION METHODS

M. Pšenička, M. Pospíšil

see page 151

L15

IN-SITU SANS STUDY OF PRECIPITATES NANOSTRUCTURE OF SINGLE CRYSTAL Ti-15Mo

V. Ryukhtin[1], P. Strunz[1], P. Kadletz[1], P. Zháňal[2], U. Keiderling[3], D. Wallacher[3]

[1]*Nuclear Physics Institute v.v.i. ASCR, 250 68 Řež, Czech Republic*

[2]*Department of Physics of Materials, Charles University, Ke Karlovu 5, 12116 Prague, Czech Republic*

[3]*Helmholtz Zentrum Berlin for Materials and Energy, D-14109 Berlin, Germany*

ryukhtin@ujf.cas.cz

Titanium alloys have plenty of applications in industry and medicine due to unique combination of high strength, low density, and excellent biocompatibility [1]. Ti-15Mo (in wt.%) is called -stabilized binary alloy, it contains mostly -phase (bcc) and also encloses metastable precipitates of (hexagonal) and (hcp) phases [2]. Microstructure of the precipitates has great impact on mechanical properties and thermal stability of the alloy. Thanks to nanometres size of the precipitates and partitioning of molybdenum content in different phases small-angle neutron scattering (SANS) instrument can be effectively used for the in-situ investigation of this microstructure.

In the present studies SANS data were measured at three orientations of the single crystal sample – (111) , (110) and (100) of -phase with correspondent plane perpendicular to incident neutron beam direction. Samples were installed in vacuum high temperature furnace and heated with heating rates of 1 K/min from room temperature up to 600 ^{0}C. SANS data were recorded in so-called list-mode and afterwards binned by time frames of 5 minutes, which corresponds to temperature range of 5 K. The measured data were calibrated using water and corrected by standard measurements of cadmium background. Scattering of the sample in high temperature furnace was used as "buffer" background.

2D pattern of SANS for sample orientation [100] parallel to incident neutron beam at temperature range 410 C ÷ 415 C taken at sample-to-detector distance SD = 12 m with collimated neutron beam of 5 Å (± 0.5 Å) wavelength is shown in Figure 1. The observed reflexions are formed by interparticles structure factor, due to high ordering of -precipitates. This ordered microstructure exists in wide

temperatures range (up to about 560 C), however the reflexions were observed in limited Q-range due to fixed SD and wavelength of the instrument. With increasing of temperature positions of the peaks decrease. Mean interparticle distances obtained from peak positions and intensities for [110] at SD = 16 m is shown in Figure 2.

Observed spots at SANS patterns at temperatures lower than about 560 C were formed by so-called isothermal iso precipitates. Symmetry of the interpaticles peaks corresponded to simple cubic ordering of the particles and basis axis are parallel to bcc axis of -phase. Increasing of temperature leads to exponential growth of volume fraction of the precipitates and increasing of interparticle distance due to coalescence of smaller precipiates into larger ones.

Scattering from iso phase became invisible at maximum instrumental resolution (SD = 16 m) after temperature exceeded 560 C due to strong intensities from very long particles. Time resolved SANS by cooling from 600 C have showed that precipitates structure do not change significantly and iso particles were not observed.

The presented investigations were supported by CSF project 14-36566G: Multidisciplinary research centre for advanced materials. Allocation of neutron beamtime at SANS instrument V4 is acknowledged to HZB.

1. Lutjering G, Williams JC (2007) *Titanium. Engineering materials, processes.* Springer, Berlin, pp 1–39. doi:10.1007/978-3-540-73036-1.

2. B.S. Hickman, *The Formation of Omega Phase in Titanium and Zirconium Alloys: A Review J. Mater. Sci.* **4 (6)** (1969) 554.

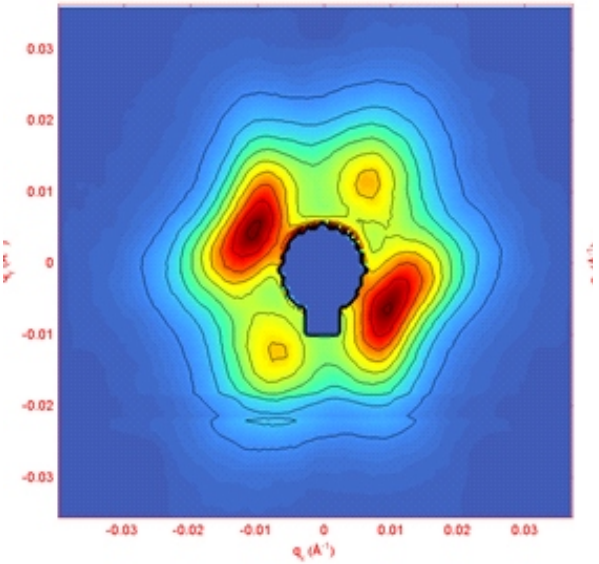

Figure 1. SANS pattern of Ti-15Mo sample in [100] orientation for temperature range 410 C ÷ 415 C during in-situ mea-

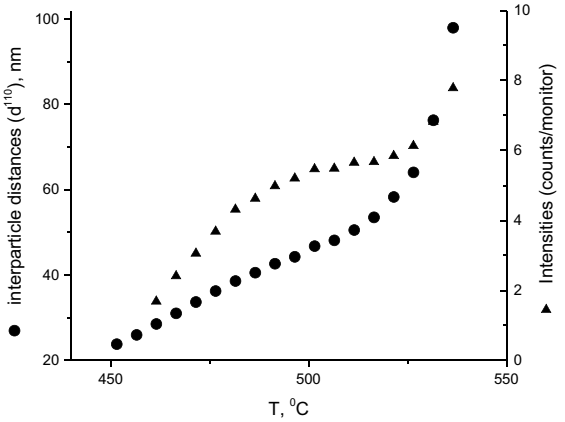

Figure 2. Interparticle distances (circles) and intensities (triangles) of peaks for [110] sample orientation in dependence on sample temperature.

L16

INCOMMENSURATELY MODULATED CRYSTAL STRUCTURES AND PHASE TRANSITIONS OF $Cu_{3+x}Si$

Cinthia Antunes Correa[1,2], Morgane Poupon[1], Jaromír Kopeček[1], Robert Král[1], Petra Zemenová[1], Jérôme Lecourt[3], Nicolas Barrier[3], Olivier Perez[3], Petr Brázda[1], Mariana Klementová[1], Lukáš Palatinus[1]

[1]Institute of Physics of the CAS, v.v.i., Na Slovance 2, 182 21 Prague 8, Czechia
[2]Department of Physics of Materials, Charles University in Prague, Ke Karlovu 5, Prague 2, Czechia
[3]CRISMAT, Normandie Universit, UNICAEN, 6Bd Marechal Juin, Caen, France
cinthiacac@gmail.com

The region with approximate composition $Cu_{3+x}Si$ of the phase diagram of Cu-Si undergoes two phase transitions with increasing temperature: ” at room temperature, ’ and at high temperature [1]. Even though the phase diagram is well established, recent studies have revealed new aspects from both the phase transitions and the crystal structures [2,3]. In this work we prepared samples by arc-melting with nominal composition $Cu_{77}Si_{23}$, $Cu_{76}Si_{24}$ and $Cu_{75}Si_{25}$. Samples were annealed at 650 °C during 24 h for homogenization. Temperature-dependent powder X-ray diffraction (TD-PXRD), temperature-dependent single crystal X-ray diffraction (TD-SCRXD), and DSC between 30 °C and 700 °C were combined for elucidating the crystal structures of the $Cu_{3+x}Si$ phases. Six phases were observed with increasing temperature: ’’’, ’’, ’, 3, 2 and 1. Five of the observed phases are incommensurately modulated. Sample $Cu_{76}Si_{24}$ was used during the temperature-dependent SCXRD. The average structure at room temperature has unit cell parameters a = 4.0700(3) Å, c = 14.6848(7) Å, it is similar for the three compositions

studied and for ''' and ″. Although the point group of the complete diffraction pattern is $\bar{3}$, the average structure can be described in the space group $P6_3/mmc$. The average structure can be described by three repetitions of hexagonal and honeycomb shaped layers (Fig. 1a). The modulation is revealed by large anisotropic distribution of electron density around the Cu atoms of the layer B. Two modulation vectors are necessary to index the complete diffraction pattern (Fig. 1b): $q_1 = (\ , \ , 1/3)$ and $q_2 = (\ , \ , 1/3)$, where $= \ = 0.2509(10)$ (point group $\bar{3}m$) for ″, and $= 0.23458(7), \ = 0.28171(7)$ (point group $\bar{3}$) for '''. Both structures could be solved in (3+2)D superspace by Superflip [4], superspace groups $P\bar{3}1c(\ , \ , 1/3)(\ , \ , 1/3)$ and $P\bar{3}(\ , \ , 1/3)(\ , \ , 1/3)$ for ' and ''', respectively. The modulation function of both structures have amplitudes comparable to the size of the unit cell, discontinuities and windows. Given the complexity of the modulation and the small number of reflections measured, the function could not be parametrized to be refined using the superspace formalism, and a supercell approximation had to be used. Since $\sim 1/4$ for '', a 4 4 3 supercell could be used, while the smallest possible approximation for ''' was a 14 14 3 supercell. The refinement was performed in Jana2006 [5].

Temperature-dependent powder X-ray diffraction of the samples $Cu_{74}Si_{26}$ and $Cu_{78}Si_{22}$ was measured every 30 °, from 30 °C to 700 °C with heating rate of 5 °C/min. Two cycles of heating and cooling were measured to verify the reversibility of the transitions. Three additional phases, which were not present in the phase diagram, were observed, the transitions were reversible and reproducible with small hysteresis in the transition temperatures. Le Bail fitting of the powder patters was performed in Jana2006 using the models obtained by SCXRD, pseudo-Voigt profile, manual background combined with fifteen terms of Legendre polynomials. Initially the main reflections were indexed using cyclic refinement, and the modulation vectors were refined separately for each temperature, after the cyclic refinement. Except for the phase 3, powder patterns of the sample $Cu_{78}Si_{22}$ presented the same transitions as for the sample $Cu_{74}Si_{26}$ and only this sample will be shown. From the six phases observed in the sample $Cu_{74}Si_{26}$, five were completely indexed. Our study shows that the phase diagram might be more complex than that reported in the literature.

1. Olesinki, R.W., Abbaschian, G.J., Bull. Alloy Phase Diagrams 7, 170 (1986).
2. Corręa C.A. et al., Acta Crystallographica B73, 767-774 (2017).
3. Corręa C.A. et al., Intermetallics 91, 129-139 (2017).
4. Palatinus, L. and Chapuis, G., J. Appl. Cryst. 40, 786–790 (2007).
5. Petříček V., Dušek M., Palatinus L., Z. Krist. 229 (5) 345–352 (2014).

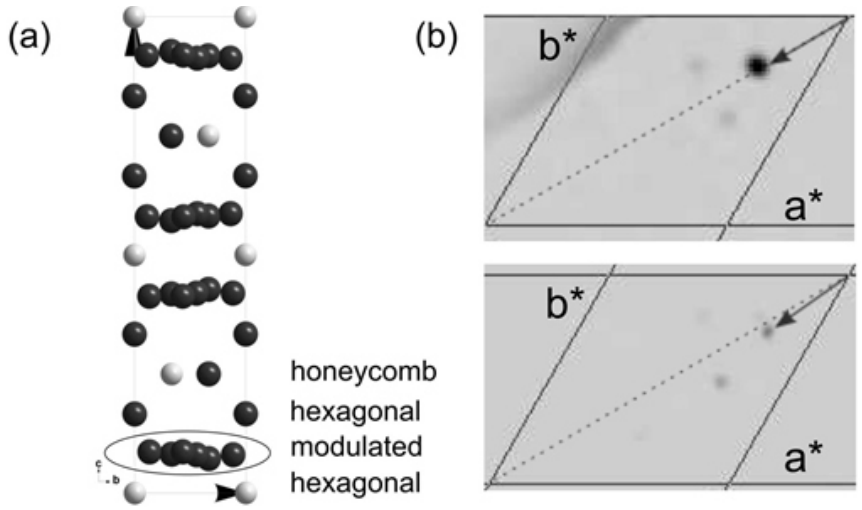

Figure 1. (a) Cu_3Si structure viewed along **a** - Cu - black, Si - grey. Strongly modulated honeycomb layer filled with copper causes two variants of the structure shown in (b) above, modulation vectors for '' q1 = (, , 1/3) and q2=(- , 1/3), where = 0.2509(10), and below, for ''' = 0.23458(7), = 0.28171(7).

L17

TRANSITIONS TOWARD COMPLEX ELECTRONIC STATES AND SUPERPERIODIC STRUCTURES IN $P_4W_{16}O_{56}$

Elen Duverger-Nedellec[1,2], Alain Pautrat[1], Olivier Perez[1]

[1]*Laboratoire CRISMAT, UMR 6508 CNRS, 6 Boulevard du Maréchal Juin, 14050 Caen CEDEX 4, FR*
[2]*Charles University,Faculty of Mathematics and Physics, KeKarlovu 3, 121 16 Praha 2, CZ*
elenduvergernedellec@gmail.com

The MonoPhosphate Tungsten Bronzes (MPTB) family, $(PO_2)_4(WO_3)_{2m}$, can be described by a regular intergrowth of (PO_4) tetrahedra layers and of slabs constituted by corner-sharing-(WO_6) octahedra, with a thickness depending on the m parameter. These low-dimensional oxides are known to exhibit successive transitions toward Charge Density Wave (CDW) states. These transitions are associated to lattice distortions leading to the appearance of incommensurate or commensurate structural modulations [1]. In this family, the electronic anisotropy and the density of carriers of the system can be tuned by modifying the thickness of the WO_3 slabs *i.e.* changing m. MPTB family is thus a relevant system to analyse the effect of the dimensionality on the CDW electronic instabilities. Temperature-dependant X-ray diffraction (XRD) [1] and transport measurements reported in the literature, for different terms of the family, reveal a significant change of behaviour between the terms with a low and high value of m, $m < 7$ and $m > 7$ respectively. Classical CDW transitions are reported for the low terms, characterized by a smooth resistivity jump and by the formation of clusters of tungsten in the centre of the WO_3 slabs [2]. For the high terms [3], a structural transition is observed in XRD but the electronic transport studies do not show the usual signature attributed to a CDW. Moreover, the only structural study performed on a high term in the modulated state ($m = 10$) [3] evidences anti-ferroelectric-type (AFE) atomic displacements for the tungsten atoms without reporting of the formation of clusters of tungsten.

We will present both the transport properties and the analysis of the structural modulations for the $m = 8$ term. Three first-order transitions associated with large thermic hysteresis were identified. The analysis of the structural modulations characterizing the different states, *via* the use of the super-space formalism, reveals the existence of AFE-type displacements and the formation of clusters for the tungsten atoms. These signatures can be assigned to the coexistence of AFE and CDW properties in the material. These two properties are *a priori* incompatible, but an extensive study of the transport properties versus temperature supports this hypothesis. This result enlightens the very interesting position of $P_4W_{16}O_{56}$ ($m = 8$) in the border area between the low and the high m values in the MPTB family to discuss the competition regime between CDW and ferroelectric instabilities.

1. A. Ottolenghi, J. P. Pouget, *J. Phys. I France*, **1996**, Vol 6, p. 1059-1083.
2. J. Lüdecke, A. Jobst, S. Van Smaalen; *Europhys.Lett*., **2000**, Vol.49, n°3, p.357–361.
3. P. Roussel et al., Phys. Rev. B, **2000**, Vol.62, p.176.